ISSN 1070-3284, Russian Journal of Coordination Chemistry, 2021, Vol. 47, No. 10, pp. 687–694. © Pleiades Publishing, Ltd., 2021.
Russian Text © The Author(s), 2021, published in Koordinatsionnaya Khimiya, 2021, Vol. 47, No. 10, pp. 620–627.

Cobalt(III) Bis-*o*-semiquinone Complexes with 1-Aryl-3,5-diphenylformazan Ligands: Synthesis, Structures, and Magnetic Properties

N. A. Protasenko[a], *, A. I. Poddelskii[a], R. V. Rumyantsev[a], I. A. Yakushev[b, c], and V. K. Cherkasov[a]

[a] *Razuvaev Institute of Organometallic Chemistry, Russian Academy of Sciences, Nizhny Novgorod, Russia*
[b] *Kurnakov Institute of General and Inorganic Chemistry, Russian Academy of Sciences, Moscow, 119991 Russia*
[c] *Kurchatov Institute Russian Research Center, Moscow, 123182 Russia*
**e-mail: tessun@yandex.ru*

Received February 11, 2021; revised April 26, 2021; accepted April 27, 2021

Abstract—New heteroligand cobalt(III) bis-3,6-di-*tert*-butyl-*o*-benzosemiquinone complexes with 1-(*p*-X-phenyl)-3,5-diphenylformazan ligands $Co(3,6\text{-}SQ)_2L^X$ (X is fluorine (**I**), chlorine (**II**), bromine (**III**), iodine (**IV**), and methyl (**V**)) are synthesized. The molecular structures of compounds **I**, **II**, and **IV** are determined by X-ray structure analysis (CIF files CCDC nos. 2060727 (**I**), 2052592 (**II**), and 2060728 (**IV**)). The coordination environment of the central cobalt ion in the studied complexes is a weakly distorted octahedron, and the degree of distortion insignificantly changes depending on the substituent. According to the X-ray structure data and results of magnetic and spectral studies, compounds **I**–**V** are low-spin complexes of cobalt(III) bound to two radical anion *o*-semiquinone ligands and one formazan anion. The magnetic behavior of complexes **I**–**V** in a temperature range of 50–300 K is characterized by the predomination of intramolecular exchange interactions of the antiferromagnetic type, whereas in the range lower than 50 K complexes **II**–**V** exhibit ferromagnetic ordering caused by intermolecular exchange interactions between the paramagnetic ligands.

Keywords: cobalt(III) complexes, *o*-semiquinone, formazan, X-ray structure analysis, magnetochemistry
DOI: 10.1134/S1070328421100067

INTRODUCTION

The development and design of heterospin systems based on coordination compounds of transition metals with stable organic radicals are among the urgent trends of the modern chemistry. The presence of several paramagnetic centers in the molecules induces increased interest in their magnetic properties, since these compounds are convenient objects for studying fine exchange interactions, whose character can be controlled by the molecular geometry, nature of substituents, steric factors, and other factors [1–10]. The transition metal complexes with radical organic ligands are actively studied as potential structural units for the construction of molecular magnetics. The coordination compounds bearing the redox-active ligands based on *o*-quinone are among the perspective classes of compounds in this field of research. The *o*-semiquinone complexes of transition metals well recommended themselves as model systems for studying metal–ligand and ligand–ligand fine magnetic interactions. Such phenomena as redox isomerism (intramolecular electron transfer) and spin crossover were found for these complexes [11, 12]. The unique properties of complexes of this type are determined by the delocalization or transfer of electron (charge) between the metal and paramagnetic organic ligand along with the possibility of affecting the charge distribution in the system by the variation of the metal ion nature and redox potential of the *o*-quinone ligand or by the introduction of additional ligands in the coordination sphere of the metal [13–19]. The N-donor neutral ligands, for example, aromatic diimines (2,2'-bipyridyl [11], 1,10-phenanthroline [20, 21], and their analogs [19]), aliphatic diamines [18, 22], and pyridine derivatives [23–25] are used, as a rule, as additional ligands in these complexes. In this work, the chelating anionic ligands of the formazan class serve as N-donor ligands. It has recently been established that, on the one hand, formazans incorporated in the coordination sphere of the metal are capable of reversible reducing to form the stable radical dianion species and, on the other hand, can undergo oxidation to the formazanyl radical [26, 27]. Thus, formazans can act as redox-active ligands similarly to *o*-quinones, which provides new possibilities for their application in the coordination chemistry and design of magnetically active compounds [28]. In our previously published studies, we described the procedure for the synthesis

of the formazanate derivatives of the transition metals from the corresponding carbonyls, presented the first examples for the heteroligand mono- and bis-*o*-semiquinoneformazanate cobalt complexes based on the 1,3,5-triphenylformazan ligands, and studied their structures and magnetic and electrochemical properties [29, 30].

The results of the synthesis and spectral, magnetic, and structural studies of five new cobalt(III) bis-*o*-semiquinone complexes with the 1-(*p*-X-phenyl)-3,5-diphenylformazan ligands (X is fluorine, chlorine, bromine, iodine, and methyl) are presented in this work.

EXPERIMENTAL

3,6-Di-*tert*-butyl-*o*-benzoquinone [31], 1,3,5-triarylformazan ligands [32], and cobalt(III) tris-(3,6-di-*tert*-butyl-*o*-benzosemiquinolate [33] used in this work were synthesized according to known procedures. The solvents necessary for experiments were purified and dehydrated using standard procedures [34]. Commercially available cobalt carbonyl (≥90% Co, Sigma-Aldrich) was used as received.

IR spectra were recorded on an FSM-1201 FT-IR spectrometer (400–4000 cm^{-1}, Nujol). Elemental analysis (C, H, N) was carried out on an Elementar Vario EL cube elemental analyzer. Magnetochemical measurements were carried out at the International Tomography Center (Russian Academy of Sciences) on an MPMSXL SQUID magnetometer (Quantum Design) in the 2 to 2–310 K range in a magnetic field of 5 kOe. The paramagnetic components of the magnetic susceptibility (χ) were determined taking into account the diamagnetic contribution estimated from Pascal's constants. The effective magnetic moment (μ_{eff}) was calculated by the equation $\mu_{eff} = [3k\chi T/(N_A\mu_B^2)]^{1/2}$, where N_A, μ_B, and k are Avogadro's number, Bohr magneton, and Bolzmann constant, respectively.

Synthesis of complex $Co(3,6\text{-}SQ)_2L^F$ (I). A solution of 1-(*p*-fluorophenyl)-3,5-diphenylformazan (0.060 g, 0.18 mmol) in toluene (5 mL) was poured to a solution of tris-(3,6-di-*tert*-butyl-*o*-benzosemiquinolatecobalt(III) (0.136 g, 0.1 mmol) in toluene (10 mL). The reaction mixture was stirred at 50°C for 24 h. The solution turned dark blue. After this, the solvent was removed completely and the remained dark precipitate was recrystallized from diethyl ether at 4°C. As a result, blue-violet rhombic crystals were formed and dried in vacuo (85% yield).

For $C_{47}H_{54}N_4O_4FCo$

Anal. calcd., %	C, 69.10	H, 6.66	N, 6.86
Found, %	C, 68.85	H, 6.70	N, 6.63

IR (ν, cm^{-1}): 1597 w, 1551 w, 1500 s, 1428 s, 1414 s, 1356 m, 1343 m, 1331 m, 1308 s, 1279 s, 1233 m, 1198 s, 1150 m, 1026 w, 993 m, 976 m, 957 m, 916 w, 831 w, 806 w, 756 s, 721 m, 692 s, 679 m, 652 s, 598 w, 563 m, 528 s, 484 w.

Complexes $Co(3,6\text{-}SQ)_2L^{Cl}$ (II), $Co(3,6\text{-}SQ)_2L^{Br}$ (III), and $Co(3,6\text{-}SQ)_2L^{I}$ (IV) were synthesized from cobalt carbonyl using a described procedure [29].

Complex II: fine dark blue prismatic crystals were recrystallized from a hexane–CH_2Cl_2 (5 : 1) mixture (81% yield).

For $C_{47}H_{54}N_4O_4ClCo$

Anal. calcd., %	C, 67.74	H, 6.53	N, 6.72
Found, %	C, 67.78	H, 6.61	N, 6.70

IR (ν, cm^{-1}): 1657 w, 1601 m, 1551 m, 1480 m, 1424 m, 1414 m, 1366 m, 1358 m, 1343 m, 1329 m, 1306 s, 1280 s, 1196 s, 1090 m, 1026 w, 1015 w, 991 w, 976 m, 957 m, 914 w, 829 s, 762 s, 721 s, 694 s, 677 m, 652 m, 636 w, 567 w, 547 w, 505 w, 482 w.

Complex III: fine dark blue prismatic crystals were recrystallized from pentane (83% yield).

For $C_{47}H_{54}N_4O_4BrCo$

Anal. calcd., %	C, 64.31	H, 6.20	N, 6.38
Found, %	C, 64.47	H, 6.31	N, 6.18

IR (ν, cm^{-1}): 1601 w, 1551 w, 1424 s, 1358 m, 1345 m, 1331 m, 1308 s, 1281 s, 1194 s, 1071 w, 1026 w, 1013 w, 991 w, 976 m, 959 m, 914 w, 897 w, 827 s, 810 w, 760 s, 721 w, 694 s, 675 w, 652 m, 632 w, 565 w, 544 w, 503 w, 484 m.

Complex IV: blue-violet needle-like crystals were recrystallized from a hexane–pentane (1 : 1) mixture (85% yield).

For $C_{47}H_{54}N_4O_4ICo$

Anal. calcd., %	C, 61.04	H, 5.89	N, 6.06
Found, %	C, 61.15	H, 6.06	N, 5.86

IR (ν, cm^{-1}): 1601 m, 1565 w, 1551 s, 1424 s, 1358 s, 1348 s, 1331 s, 1279 s, 1198 s, 1171 w, 1155 w, 1101 w, 1078 w, 1055 w, 1028 m, 1007 s, 991 s, 976 s, 957 s, 914 m, 897 w, 827 s, 810 m, 760 s, 719 m, 694 s, 683 s, 673 m, 652 s, 632 w, 574 w, 563 w, 542 m, 528 w, 503 m, 482 m.

Complex $Co(3,6\text{-}SQ)_2L^{Me}$ (V) was synthesized using the procedure similar to that for complex **I**.

Complex V: fine dark violet cubic crystals were recrystallized from a toluene–hexane (1 : 1) mixture (86% yield).

For $C_{48}H_{57}N_4O_4Co$

Anal. calcd., %	C, 70.92	H, 7.07	N, 6.89
Found, %	C, 71.03	H, 7.15	N, 6.67

IR (ν, cm^{-1}): 1680 w, 1657 m, 1603 w, 1551 m, 1503 w, 1424 s, 1358 s, 1345 s, 1329 m, 1306 s, 1280 s, 1269 s, 1198 s, 1169 w, 1111 w, 1080 w, 1072 w, 1026 w, 993 m, 978 m, 959 s, 939 w, 918 w, 827 s, 760 s, 721 w, 695 s, 679 s, 652 s, 563 w, 530 w, 503 w, 480 m.

X-ray structure analysis (XSA). Diffraction data for crystals of compounds **I** and **IV** were collected on an Oxford Xcalibur Eos single-crystal X-ray diffractometer (ω scan mode, graphite monochromator, MoK_α radiation, λ = 0.71073 Å). Experimental sets of intensities for complexes **I** and **IV** were integrated using the CrysAlisPro software [35]. An absorption correction was applied using the SCALE3 ABSPACK algorithm [35]. The structures of compounds **I** and **IV** were solved using the SHELXT software [36] and refined by full-matrix least squares for F^2 in the anisotropic approximation for all non-hydrogen atoms using the SHELXL software [37]. All hydrogen atoms in compounds **I** and **IV**, except for H(1S*A*) and H(1S*B*) in complex **IV**, were placed in the geometrically calculated positions and refined isotropically. In turn, the H(1S*A*) and H(1S*B*) in complex **IV** were localized objectively from the difference Fourier synthesis and refined in the isotropic approximation. In the crystal of compound **IV**, 0.2 water molecule falls onto each molecule of the complex. The EADP, ISOR, and DFIX instructions were used to refine disordered fragments in complexes **I** and **IV**.

Diffraction data for crystals of compound **II** were collected on a Bruker D8 Venture Photon diffractometer in the φ and ω scan modes at the Center for Collective Use "Physical Methods of Investigation" at the Kurnakov Institute of General and Inorganic Chemistry (Russian Academy of Sciences) at 150 K (λ = 0.71073 Å, Incoatec IμS 3.0 microfocus X-ray source). The primary indexing, unit cell parameter refinement, and reflection integration were performed using the Bruker APEX3 program package [38]. An absorption correction to reflection intensities was applied using the SADABS program [38]. The structure of compound **II** was solved by direct methods and refined by full-matrix least squares for F^2 in the anisotropic approximation for all non-hydrogen atoms, except for the strongly disordered moiety of the molecule of compound **II**, carbon atoms of which were refined in the isotropic approximation. The EADP, FLAT, and SADI instructions were applied to construct an adequate model for disordering in structure refinement of compound **II**. Hydrogen atoms were placed in the calculated positions and refined by the riding model with $U_{iso}(H) = 1.5U_{equiv}(C)$ for the hydrogen atoms of the methyl groups and $1.2U_{equiv}(C)$ for other hydrogen atoms. Calculations were performed using the SHELXTL software [37] in the OLEX2 medium of structural data visualization and processing [39].

The crystallographic data and structure refinement parameters for compounds **I**, **II**, and **IV** are given in Table 1. Selected bond lengths are listed in Table 2. The structural data were deposited with the Cambridge Crystallographic Data Centre (CIF files CCDC nos. 2060727 (**I**), 2052592 (**II**), and 2060728 (**IV**); https://www.ccdc.cam.ac.uk/structures/).

RESULTS AND DISCUSSION

The series of the heteroligand hexacoordinate cobalt(III) bis-*o*-semiquinoneformazanate complexes was synthesized by the reactions shown in Scheme 1. Synthesized complexes **I**–**V** in the crystalline form are resistant to air oxygen and moisture and are easily soluble in the most part of organic solvents.

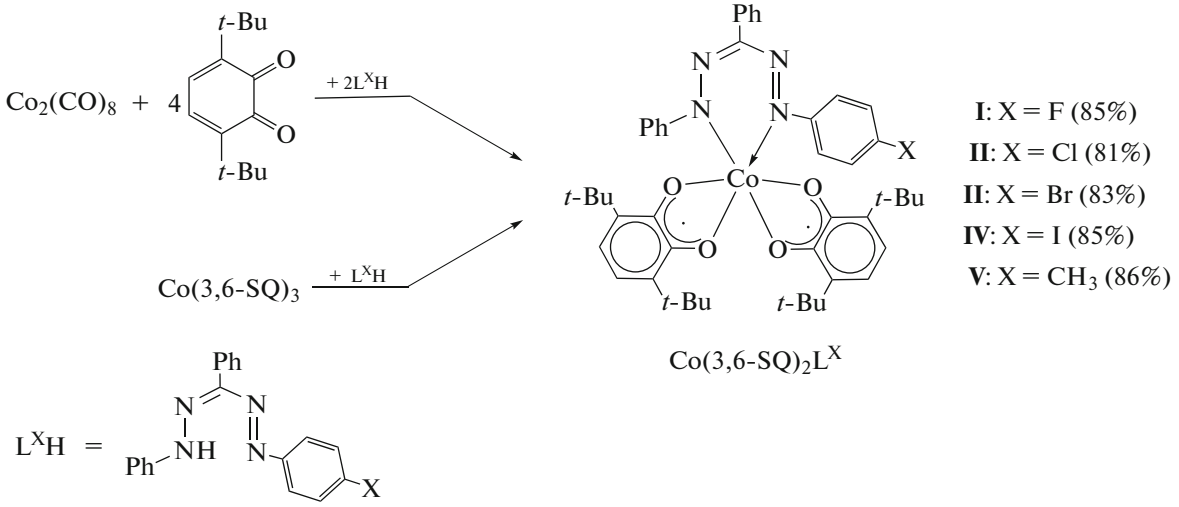

Scheme 1.

Table 1. Crystallographic data and structure refinement parameters for complexes **I**, **II**, and **IV**

Complex	**I**	**II**	**IV**
T, K	100(2)	150(2)	100(2)
Crystal system	Triclinic	Triclinic	Triclinic
Space group	$P\bar{1}$	$P\bar{1}$	$P\bar{1}$
a, Å	11.40191(19)	11.2996(10)	11.49220(10)
b, Å	12.3023(2)	14.3044(13)	12.31140(10)
c, Å	16.3713(3)	14.7495(13)	17.3415(2)
α, deg	80.5542(15)	80.230(4)	107.5340(10)
β, deg	79.0584(14)	76.916(3)	103.2140(10)
γ, deg	72.9732(16)	71.776(3)	97.4910(10)
V, Å^3	2141.38(7)	2193.0(3)	2224.54(4)
Z	2	2	2
ρ_{calc}, mg/m^3	1.267	1.262	1.386
μ, mm^{-1}	0.452	0.499	1.126
θ, deg	2.938–28.000	2.083–27.157	2.968–27.999
Number of observed reflections	39595	22028	40151
Number of independent reflections	10326	9623	10706
R_{int}	0.0435	0.0452	0.0395
$S(F^2)$	1.026	1.040	1.044
R_1, wR_2 ($I > 2\sigma(I)$)	0.0403, 0.0930	0.0589, 0.1122	0.0339, 0.0851
R_1, wR_2 (for all parameters)	0.0579, 0.0994	0.0924, 0.1239	0.0454, 0.0897
$\Delta\rho_{max}/\Delta\rho_{min}$, e Å^{-3}	0.354/–0.391	0.469/–0.504	1.128/–0.566

The compositions and structures of compounds **I**–**V** were determined from the IR spectroscopic and elemental analysis data. The IR spectra of the synthesized compounds exhibit a set of bands characteristic of the ligands of the complexes. For example, the IR spectra of complexes **I**–**V** contain bands at 1610–1540 cm^{-1} corresponding to stretching vibrations of the C=N and N=N bonds of the coordinated formazan ligands along with the intense bands caused by stretching vibrations of the C–O bonds of the *o*-semiquinone ligands (1350–1450 cm^{-1}).

The molecular structures of complexes **I**, **II**, and **IV** in the crystalline state were determined by the XSA method. As shown in Fig. 1, the molecular structures of all the three compounds are similar, and the environment of the central cobalt atom is a weakly distorted octahedron. The geometric characteristics of the *O*,*O*'-chelating dioxolene ligands are typical of the radical anion *o*-benzosemiquinone species: the C–O bond lengths range from 1.291(2) to 1.323(3) Å (Table 2), and the quinoid type of distortion is observed for the C–C bonds of the phenyl ring [40, 41]. The Co–O bond lengths in complexes **I**, **II**, and **IV** range from 1.8738(19) to 1.9198(12) Å, which are consistent with similar values for the known hexacoordinate *o*-semiquinone complexes of low-spin cobalt(III) (1.8–1.9 Å, [33, 42]) and are by ~0.1–0.2 Å shorter than similar bonds in the *o*-semiquinone complexes of high-spin cobalt(II) (2.0–2.1 Å) [42–44].

The dihedral angle between the planes of *o*-semiquinone ligands decreases in the series of compounds **I**, **II**, and **IV** and equals 80.47°, 77.91°, and 74.24°, respectively. The analogous angle in the bis-*o*-semiquinone complex with unsubstituted formazan is 77.90°.

The N–N and N–C bonds inside the chelate cycle of the formazanate ligand are delocalized, indicating the anionic form of the ligand [29, 45–47]. The N–N bond lengths range from 1.282(3) to 1.296(2) Å, and the N–C bond lengths lie in a range of 1.344(2)–1.352(3) Å (Table 2). The N(1)N(2)C(35)N(3)-N(4)Co(1) chelate cycle itself is not planar and bent along the N(1)...N(4) line in the same way as in the

Table 2. Selected bond lengths (Å) and angles (deg) in complexes **I**, **II**, and **IV**

Bond	**I**	**II**	**IV**
Co(1)–O(1)	1.8923(11)	1.8738(19)	1.8804(14)
Co(1)–O(2)	1.9066(12)	1.909(2)	1.9015(15)
Co(1)–O(3)	1.9198(12)	1.9039(19)	1.9024(15)
Co(1)–O(4)	1.9024(11)	1.8981(19)	1.9143(14)
Co(1)–N(1)	1.9021(14)	1.898(2)	1.9145(17)
Co(1)–N(4)	1.9084(14)	1.911(2)	1.8969(18)
O(1)–C(1)	1.3058(19)	1.302(3)	1.323(3)
O(2)–C(2)	1.2958(19)	1.292(3)	1.293(3)
O(3)–C(15)	1.2909(19)	1.293(3)	1.297(3)
O(4)–C(16)	1.302(2)	1.298(3)	1.313(3)
N(1)–N(2)	1.2924(19)	1.292(3)	1.296(2)
N(2)–C(35)	1.344(2)	1.346(3)	1.345(3)
N(3)–C(35)	1.345(2)	1.347(3)	1.352(3)
N(3)–N(4)	1.2895(19)	1.282(3)	1.282(2)
F(1)–C(32)	1.333(3)		
Cl(1)–C(32)		1.733(3)	
I(1)–C(32)			2.103(2)
Angle	**I**	**II**	**IV**
O(1)Co(1)O(2)	85.33(5)	85.48(8)	85.80(6)
O(3)Co(1)O(4)	84.52(5)	84.73(8)	84.88(6)
N(1)Co(1)N(4)	85.69(6)	85.24(10)	85.26(8)
N(1)Co(1)O(3)	177.48(6)	177.52(9)	175.11(7)
O(1)Co(1)O(4)	171.95(5)	171.02(9)	169.73(7)
O(2)Co(1)N(4)	175.15(5)	173.09(9)	175.37(7)

cobalt bis-*o*-semiquinone complex with unsubstituted 1,3,5-triphenylformazan [29]. Note that owing to the mutual repulsion of the substituents the bent angle of the metallocycle in complexes **I**, **II**, and **IV** with 1-(*p*-X-phenyl)-3,5-diphenylformazan ligands is by several degrees higher than that in analogous complex with unsubstituted formazan, being 37.73° for **I**, 39.88° for **II**, and 39.89° for **IV**, respectively. The phenyl substituents at the N(1) and N(5) atoms of the formazan ligand in complexes **I** and **II** are turned relative to the plane of the azohydrazone chain by an angle of ~45°. Asymmetry in the arrangement of the indicated substituents is observed for compound **IV**: for example, the unsubstituted phenyl ring at the N(4) atom is arranged at an angle of 46.64° to the plane of the formazanate carcass, whereas the phenyl ring at the N(1) atom with the iodine substituent in the *para* position is turned by 33.01°, which can be associated with the crystal packing of the molecules and intermolecular interactions between the iodine atoms of the adjacent molecules of the complex. The corresponding I–I distance is 4.334 Å (Fig. 2), which only insignificantly exceeds the sum of van der Waals radii of two iodine atoms (4.2 Å [48]).

Thus, the introduction of the halogen atom in the *para* position of the phenyl substituent at the N(1) atom of the formazanate ligand insignificantly affects the molecular structures and geometry of the formed mixed-ligand complexes.

The magnetic properties of complexes **I**–**V** in the 2 to 300 K temperature range were studied. The temperature dependences of the effective magnetic moment for these complexes are shown in Fig. 3. The high-temperature value of μ_{eff} for complex **I** is 2.68 μ_B

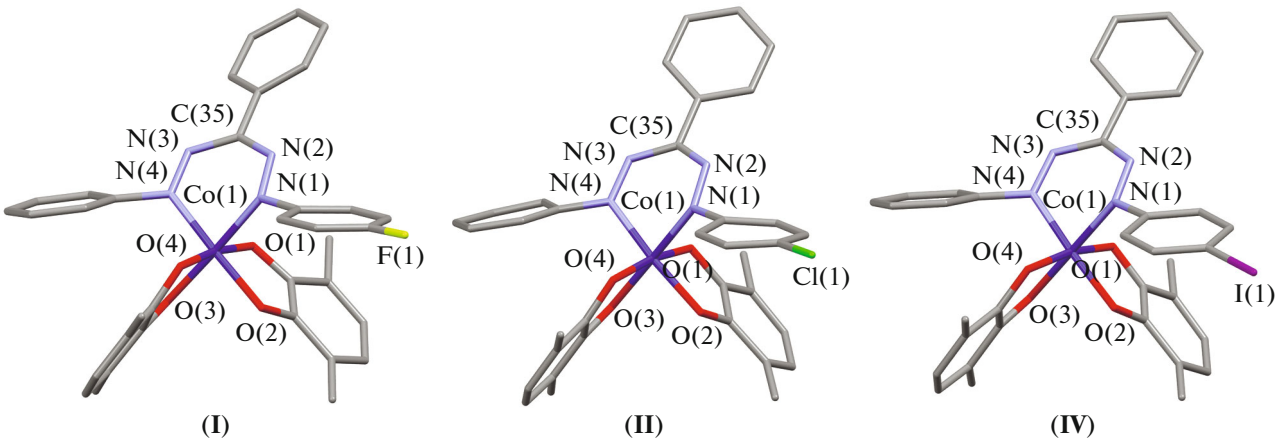

Fig. 1. Molecular structures of complexes **I**, **II**, and **IV** according to the XSA data. The methyls of the *tert*-butyl groups and hydrogen atoms are omitted.

(300 K), which is insignificantly higher than the spin-only value equal to 2.45 μ_B calculated for the system consisting of two radical centers with $S = 1/2$ for each center. This state of the system is possible for the Co(III) complex bound to two radical anion *o*-semiquinone ligands and one formazanate anion. As the temperature decreases, the magnetic moment first decreases smoothly in a range of 300–100 K and then decreases more sharply to 0.66 μ_B at 2 K, which indicates the antiferromagnetic character of the exchange between the radical centers. A similar behavior is observed for the cobalt(III) bis-*o*-semiquinone complex with unsubstituted 1,3,5-triphenylformazanate [29].

The high-temperature value of the effective magnetic moment (300 K) for complexes **II**–**V** is also close to the value for the spin system consisting of two radical centers with $S = 1/2$. The value of μ_{eff} for these complexes decreases smoothly with decreasing temperature in a range of 300–50 K. This behavior is characteristic of the biradical systems with the antiferromagnetic type of intramolecular exchange interactions. Unlike complex **I**, some increase in μ_{eff} is observed with the further decrease in temperature. For example, some increase in the effective magnetic moment is observed only at the temperatures lower than 25 K for complexes **II** and **III**, whereas for compounds **IV** and **V** the increase starts already after 50 K. The maximum jump of μ_{eff} is observed for complex **IV** (Fig. 3, curve ▼). In this case, μ_{eff} decreases smoothly with decreasing temperature from 2.37 μ_B at 300 K to 1.31 μ_B at 50 K, then increases to 1.9 μ_B at 25 K, and on further cooling decreases sharply 0.48 μ_B at 2 K. This behavior of the complexes at low temperatures can probably be related to the ferromagnetic spin ordering in the radical *o*-semiquinone ligands of the adjacent molecules in the crystal packing of the complex. An analysis of the structural data available at the moment shows that in crystals the molecules of these complexes are packed in beveled stacks, and the paramagnetic *o*-semiquinone ligands from the adjacent stacks are facing to each other and parallel (Fig. 2). For complex **IV** with the highest jump of the magnetic moment, the least distance between the *o*-semiquinone ligands of the adjacent molecules is the shortest and equal to 4.170 Å, whereas this distance is the longest and equal to 4.661 Å for complex **I** in which no jump is observed. This value is 4.299 Å in complex **II** in which an insignificant increase in the magnetic moment is observed at low temperatures, and this distance is 4.556 Å for the previously published complex with unsubstituted 1,3,5-triphenylformazan [29], where no ferromagnetic ordering occurs.

To conclude, the results of the present study show that the introduction of the substituent in the *para*-position of the phenyl ring at the N(1) atom of the formazanate ligand in the cobalt(III) bis-*o*-semiquinoneformazanate complexes affects the crystal packing of the molecules of the complex, which in turn affects the character of the intermolecular exchange interactions and magnetic behavior of the complexes at low temperatures. The magnetic properties of similar complexes will be studied in more detail elsewhere.

ACKNOWLDGMENTS

The authors are grateful to A.S. Bogomyakov (International Tomography Center, Siberian Branch, Russian Academy of Sciences) for magnetochemical measurements. Elemental analyses and IR spectroscopy of compounds **I**–**V** and XSA studies of complexes **I** and **IV** were carried out using equipment of the Center for Collective Use "Analytical Center of Institute of Organometallic Chemistry of Rus-

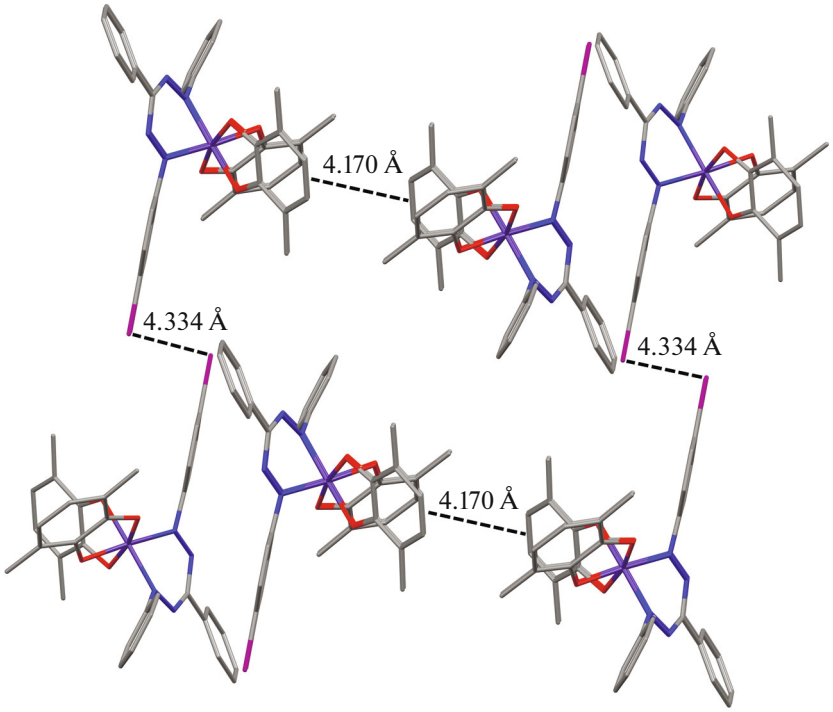

Fig. 2. Fragment of the crystal packing of complex **IV**. The methyls of the *tert*-butyl groups and hydrogen atoms are omitted.

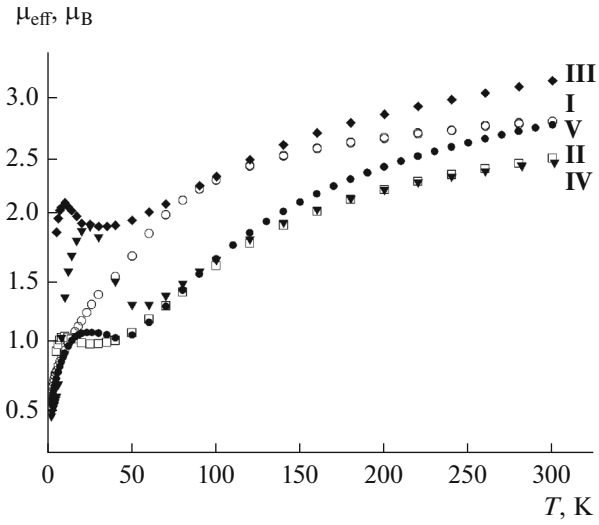

Fig. 3. Temperature dependences of the effective magnetic moments of complexes (○) **I**, (□) **II**, (◆) **III**, (▼) **IV**, and (●) **V**.

sian Academy of Sciences" at the Razuvaev Institute of Organometallic Chemistry (Russian Academy of Sciences).

The structure of complex **II** was studied in terms of state assignment of the Kurnakov Institute of General and Inorganic Chemistry (Russian Academy of Sciences) in the area of basic research.

FUNDING

This work was supported by the Russian Science Foundation, project no. 20-73-00157.

CONFLICT OF INTEREST

The authors declare that they have no conflict of interest.

REFERENCES

1. Pierpont, C.G., *Coord. Chem. Rev.*, 2001, vols. 219–221, p. 415.
2. Khusniyarov, M.M., Harms, K., Burghaus, O., et al., *Dalton Trans.*, 2008, p. 1355.
3. Poddel'sky, A.I., Cherkasov, V.K., and Abakumov, G.A., *Coord. Chem. Rev.*, 2009, vol. 253, p. 291.
4. Shultz, D.A., *Comments Inorg. Chem.*, 2010, vol. 23, no. 1, p. 1.
5. Kaim, W., Beyer, K., Filippou, V., et al., *Coord. Chem. Rev.*, 2018, vol. 355, p. 173.
6. Starikova, A.A. and Minkin, V.I., *Russ. Chem. Rev.*, 2018, vol. 87, no. 11, p. 1049.
7. Ershova, I.V., Piskunov, A.V., and Cherkasov, V.K., *Russ. Chem. Rev.*, 2020. vol. 89, no. 11, p. 1157.
8. Protasenko, N.A. and Poddel'sky, A.I., *Theor. Exp. Chem.*, 2020, vol. 56, no. 5, p. 338.
9. Perfetti, M., Caneschi, A., Sukhikh, T.S., et al., *Inorg. Chem.*, 2020, vol. 59, no. 22, p. 16591.
10. Starikova, A.A., Chegerev, M.G., and Starikov, A.G., *Chem. Phys. Lett.*, 2021, vol. 762, p. 138128.

11. Abakumov, G.A., Cherkasov, V.K., Bubnov, M.P., et al., *Dokl. Ross. Akad. Nauk*, 1993. vol. 328, p. 332.
12. Sato, O., Tao, J., and Zhang, Yu.-Z.H., *Angew. Chem., Int. Ed.*, 2007, vol. 46, p. 2152.
13. Pierpont, C.G., *Coord. Chem. Rev.*, 2001, vols. 216–217, p. 99.
14. Jung, O.-S., Jo, D.H., Lee, Y.-A., et al., *Angew. Chem., Int. Ed.*, 1996, vol. 35, p. 1694.
15. Jung, O.-S., Lee, Y.-A., Park, S.H., et al., *Bull. Chem. Soc. Jpn.*, 2001, vol. 74, p. 305.
16. Attia, A.S., Bhattacharya, S., and Pierpont, C.G., *Inorg. Chem.*, 1995, vol. 34, p. 4427.
17. Imaz, I., Maspoch, D., Rodriguez-Blanco, C., et al., *Angew. Chem., Int. Ed.*, 2008, vol. 47, p. 1857.
18. Hui, L., Young Mee, N., In Sung C., et al., *Bull. Chem. Soc. Jpn.*, 2007, vol. 80, p. 916.
19. Bin-Salamon, S., Brewer, S.H., Depperman, E.C., et al., *Inorg. Chem.*, 2006, vol. 45, p. 4461.
20. Adams, D.M., Dei, A., Rheingold, A.L., et al., *J. Am. Chem. Soc.*, 1993, vol. 115, p. 8221.
21. Bubnov, M.P., Skorodumova, N.A., Bogomyakov, A.S., et al., *Russ. Chem. Bull.*, vol. 60, p. 449.
22. Jung, O.-S., Jo, D.H., Lee, Y.-A., et al., *Inorg. Chem.*, 1998, vol. 37, p. 5875.
23. Kiriya, D., Chang, H.-C., Nakamura, K., et al., *Chem. Mater.*, 2009, vol. 21, p. 1980.
24. Schmidt, R.D., Shultz, D.A., Martin, J.D., et al., *J. Am. Chem. Soc.*, 2010, vol. 132, p. 6261.
25. Witt, A., Heinemann, F.W., Sproules, S., et al., *Chem.-Eur. J.*, 2014, vol. 20, p. 11149.
26. Chang, M.-C., Dann, T., Day, D.P., et al., *Angew. Chem., Int. Ed.*, 2014, vol. 53, p. 4118.
27. Maar, R.R., Barbon, S.M., Sharma, N., et al., *Chem.-Eur. J.*, 2015, vol. 21, p. 15589.
28. Gilroy, J.B. and Otten, E., *Chem. Soc. Rev.*, 2020, vol. 49, p. 85.
29. Protasenko, N.A., Poddel'sky, A.I., Bogomyakov, A.S., et al., *Inorg. Chem.*, 2015, vol. 54, p. 6078.
30. Protasenko, N.A., Poddel'sky, A.I., Bogomyakov, A.S., et al., *Inorg. Chim. Acta*, 2019, vol. 489, p. 1.
31. Belostotskaya, I.S., Komissarova, N.L., Dzhuaryan, Z.V., et al., *Izv. Akad. Nauk SSSR, Ser. Khim.*, 1972, no. 7, p. 1594.
32. Ashley, J.N., Davis, B.M., Nineham, A.W., et al., *J. Chem. Soc.*, 1953, p. 3881.
33. Lange, C.W., Couklin, B.J., and Pierpont, C.G., *Inorg. Chem.*, 1994, vol. 33, p. 1276.
34. Gordon, A.J. and Ford, R.A., *The Chemist's Companion*, New York: Wiley, 1972.
35. *Rigaku Oxford Diffraction. CrysAlis Pro Software System. Version 1.171.37.35*, Wroclaw: Rigaku Corporation, 2014.
36. Sheldrick, G.M., *Acta Crystallogr., Sect. A: Found. Adv.*, 2015, vol. 71, p. 3.
37. Sheldrick, G.M., *Acta Crystallogr., Sect. C: Struct. Chem.*, 2015, vol. 71, p. 3.
38. *APEX3. SAINT and SADABS*, Madison: Bruker AXS Inc., 2016.
39. Dolomanov, O.V., Bourhis, L.J., Gildea, R.J., et al., *J. Appl. Crystallogr.*, 2009, vol. 42, p. 339.
40. Brown, S.N., *Inorg. Chem.*, 2012, vol. 51, no. 3, p. 1251.
41. Pavlova, N.A., Poddel'sky, A.I., Bogomyakov, A.S., et al., *Inorg. Chem.* Commun, 2011, vol. 14, no. 10, p. 1661.
42. Dai, J., Kanegawa, S., Li, Z., Kang, S., and Sato, O., *Eur. J. Inorg. Chem.*, 2013, p. 4150.
43. Protasenko, N.A., Poddel'sky, A.I., Bogomyakov, A.S., et al., *Polyhedron*, 2013, vol. 49, p. 239.
44. Zolotukhin, A.A., Bubnov, M.P., Arapova, A.V., et al., *Inorg. Chem.*, 2017, vol. 56, p. 14751.
45. Dale, D., *J. Chem. Soc. A*, 1967, p. 278.
46. Siedle, A.R. and Pignolet, L.H., *Inorg. Chem.*, 1980, vol. 19, p. 2052.
47. Gilroy, J.B., Patrick, B.O., McDonald, R., et al., *Inorg. Chem.*, 2008, vol. 47, p. 1287.
48. Batsanov, S.S., *Inorg. Mater.*, 2001, vol. 37, no. 9, p. 871.

Translated by E. Yablonskaya